



Cite this: *Chem. Commun.*, 2016, 52, 11524

Received 22nd July 2016,  
Accepted 19th August 2016

DOI: 10.1039/c6cc06070f

www.rsc.org/chemcomm

**Memory effects in Li-ion battery materials have been explained on the basis of the thermodynamics of many-particles body, however the role of the (de-)intercalation kinetics is not yet clear. We demonstrate that kinetic aspects, specifically Li-ion mobility, are determining the magnitude of the memory effect in TiO<sub>2</sub> by studying samples with different levels of oxygen vacancies.**

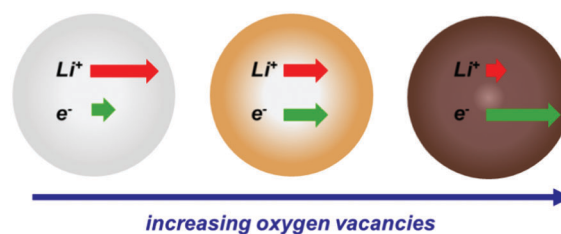
In batteries such as Ni–Cd or Ni–MH the (dis-)charge potential profile is influenced by their history. In other words, these batteries “memorize” the history of (dis-)charge, *e.g.* depth of charge or discharge in previous cycles, and they behave differently according to that history.<sup>1–3</sup> This effect has critical consequences on the performance of a battery as it interferes with the readings of the state of charge (SOC). This issue was believed to be overcome in Li-ion batteries (LIBs) since intercalation materials were reported not to suffer from memory effects, which was seen as one of the advantages of LIBs.<sup>4</sup> However, Sasaki *et al.* revealed the presence of a memory effect in LiFePO<sub>4</sub> which is one of the most widely used battery material.<sup>5</sup> This phenomenon was also detected in other intercalation materials, *i.e.* TiO<sub>2</sub> and Al-doped Li<sub>4</sub>Ti<sub>5</sub>O<sub>12</sub>.<sup>6,7</sup> So far, little is known about the origin and mechanism of the memory effect in intercalation materials. In a first attempt, the memory effect was hypothesized to originate from the particle-by-particle charging process, which derives from the two-phase (Li-rich and Li-poor) equilibrium of LiFePO<sub>4</sub>. This proposed mechanism was entirely based on the thermodynamics of intercalation materials, and could not properly explain empiric observations such as a dependence of the magnitude of the

## Understanding memory effects in Li-ion batteries: evidence of a kinetic origin in TiO<sub>2</sub> upon hydrogen annealing†

E. Ventosa,<sup>\*a</sup> T. Löffler,<sup>a</sup> F. La Mantia<sup>bc</sup> and W. Schuhmann<sup>a</sup>

memory effect on the particle size of TiO<sub>2</sub>,<sup>6</sup> or the appearance of a memory effect upon Al-doping in Li<sub>4</sub>Ti<sub>5</sub>O<sub>12</sub>.<sup>7</sup> Here, we investigate the kinetic origin of the memory effect in LIBs using anatase TiO<sub>2</sub> as model material, specifically the influence of the Li-ion mobility in the intercalation material on the memory effect.

The high operating potential of TiO<sub>2</sub> (*ca.* 1.8 V vs. Li/Li<sup>+</sup>) reduces the cell voltage and consequently the energy density of the resulting battery. However, it offers several advantages. The large voltage gap to Li electroplating enhances the safety, while the absence of a thick SEI increases the cyclability.<sup>8,9</sup> The latter also makes TiO<sub>2</sub> a good model material due to its relatively simple solid-liquid interface. The slow kinetics of Li-ion (de-)intercalation in TiO<sub>2</sub> impede achieving its theoretical specific charge of 336 mA h g<sup>-1</sup> at moderate C-rates (>0.1C). Both Li-ion and electron conductivities in TiO<sub>2</sub> are relatively low as compared to other intercalation materials. Many strategies have been reported to improve the kinetics of (de-)intercalation in TiO<sub>2</sub>.<sup>9</sup> Introducing oxygen vacancies (TiO<sub>2-x</sub>) by hydrogen annealing of anatase TiO<sub>2</sub> has been demonstrated to be an effective and simple approach.<sup>10–13</sup> Specifically, the electron mobility is enhanced with increasing levels of oxygen vacancies while Li-ion mobility decreases, as illustrated in Scheme 1.<sup>10</sup> As a result, the kinetics of (de-)intercalation improve with increasing levels of oxygen vacancies until reaching a maximum. After that, the decrease in Li-ion mobility outweighs the increase in electron mobility.<sup>10</sup> The changes in (de-)intercalation kinetics upon



**Scheme 1** Illustration of the changes in electron and Li-ion mobility in TiO<sub>2</sub> upon increasing oxygen vacancies. Adapted with permission from ref. 10.

<sup>a</sup> Analytical Chemistry – Center for Electrochemical Sciences (CES), Ruhr-Universität Bochum, D-44780 Bochum, Germany.  
E-mail: edgar.ventosa@rub.de

<sup>b</sup> Semiconductor and Energy Conversion – Center for Electrochemical Sciences (CES), Ruhr-Universität Bochum, Universitätsstr. 150, D-44780 Bochum, Germany

<sup>c</sup> Energiespeicher- und Energiewandlersysteme, Universität Bremen, Wiener Str. 12, 28359 Bremen, Germany

† Electronic supplementary information (ESI) available: Details about the chemicals, the sample preparation, the electrochemical measurements, XRD patterns and UV-Vis spectra. See DOI: 10.1039/c6cc06070f



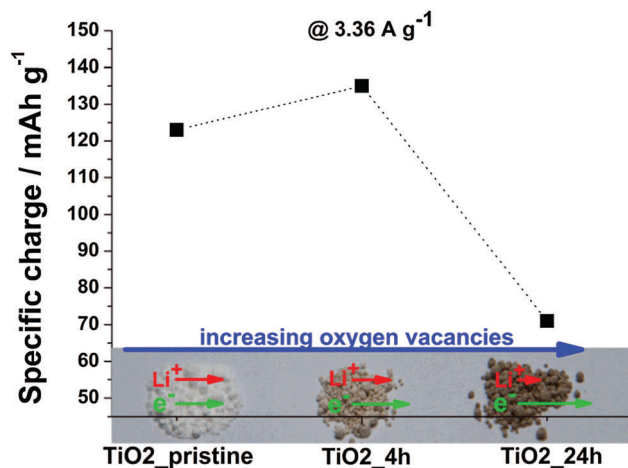


Fig. 1 Specific charge at  $3.36 \text{ A g}^{-1}$  (theoretical C-rate of 10 C) as well as photograph of  $\text{TiO}_2$ \_pristine,  $\text{TiO}_2$ \_4 h and  $\text{TiO}_2$ \_24 h.

introduction of oxygen vacancies are used in this work to elucidate the effect of (de-)intercalation kinetics on the memory effect.

Commercially available anatase  $\text{TiO}_2$  ( $\text{TiO}_2$ \_pristine) was annealed in  $\text{H}_2$  at  $300^\circ\text{C}$  for 4 h ( $\text{TiO}_2$ \_4 h) and 24 h ( $\text{TiO}_2$ \_24 h). X-ray diffraction (XRD) of  $\text{TiO}_2$ \_24 h ruled out the appearance

of new crystal phase even after annealing for 24 h (see ESI,† Fig. S1a). All three samples possessed high specific surface areas ( $>200 \text{ m}^2 \text{ g}^{-1}$ ), namely,  $300 \text{ m}^2 \text{ g}^{-1}$ ,  $220$  and  $210 \text{ m}^2 \text{ g}^{-1}$  for  $\text{TiO}_2$ \_pristine,  $\text{TiO}_2$ \_4 h and  $\text{TiO}_2$ \_24 h, respectively. The darkening in the color of the samples upon prolonged annealing time (Fig. 1) indicates a gradual increase in the level of oxygen vacancies. UV-Vis spectroscopy confirmed the introduction of oxygen vacancies (see ESI,† Fig. S1b).

The specific charge delivered at high C-rates ( $3.36 \text{ A g}^{-1}$  corresponding to a theoretical C-rate of 10 C) is dependent on the kinetics of (de-)intercalation: the faster the kinetics, the higher is the specific charge. Fig. 1 shows that the kinetics in  $\text{TiO}_2$  slightly improved for the sample annealed for 4 h, but drastically decreased in case of a 24 h treatment. This trend primary derives from the introduction of oxygen vacancies in  $\text{TiO}_2$  upon  $\text{H}_2$  annealing, as shown in previous reports.<sup>10–12</sup> The specific charge increases from  $\text{TiO}_2$ \_pristine to  $\text{TiO}_2$ \_4 h due to the increased electric conductivity and it decreases for prolonged annealing time ( $\text{TiO}_2$ \_24 h) since the decrease in Li-ion mobility outweighs the increase in electric conductivity.<sup>10</sup> The contribution of the changes in specific surface area to the trend is negligible (see ESI† for further discussion).

An electrochemical protocol was used to determine the presence and magnitude of memory effect.<sup>5–7</sup> The protocol consisted of

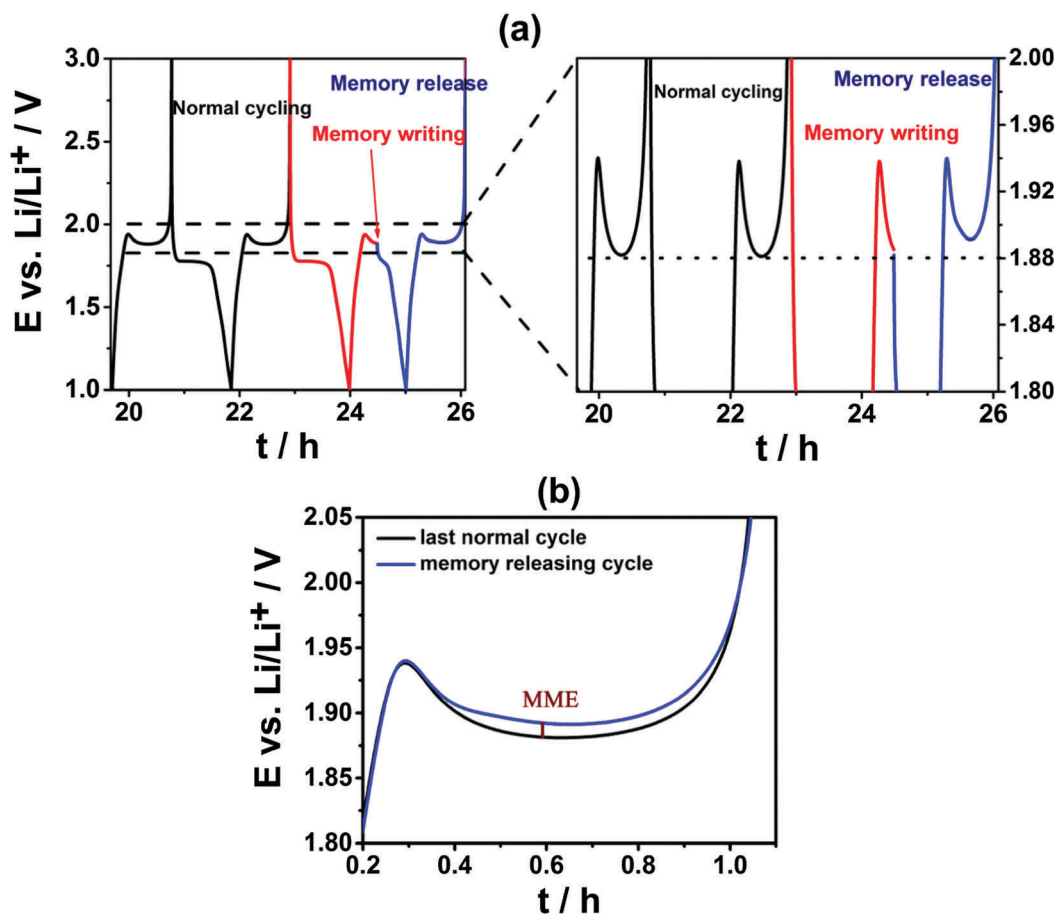


Fig. 2 (a) Potential profile of  $\text{TiO}_2$  during the three subsequent cycles required for the determination of the magnitude of the memory effect (MME). (b) Superimposed potential profiles of a normal cycle and a memory releasing cycle.



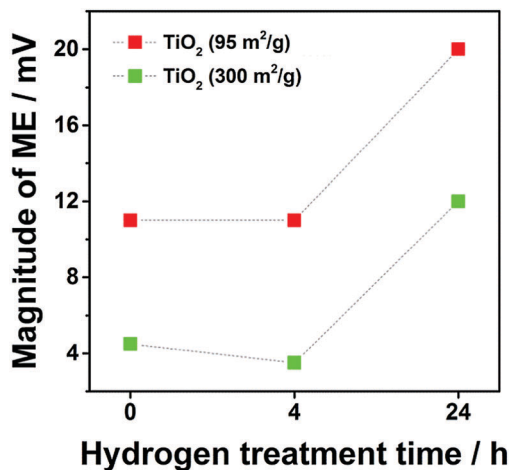


Fig. 3 Dependence of the magnitude of the memory effect (MME) on the duration of H<sub>2</sub> annealing time (pristine, 4 h and 24 h) for two commercial TiO<sub>2</sub> samples with 300 m<sup>2</sup> g<sup>-1</sup> in green and with 95 m<sup>2</sup> g<sup>-1</sup> in red. The potential profiles of all samples are shown in Fig. S2 (ESI†).

applying three subsequent cycles: a normal (de-)intercalation cycle, a memory writing cycle and a memory releasing cycle (Fig. 2a). During the memory writing cycle, the anodic process was interrupted at a certain SOC. In the next memory releasing step, the sample was cycled within the normal potential range, and the memory effect was revealed if occurred. It appeared as a bump in the plateau on Li-ion de-intercalation occurring at a similar SOC at which the memory writing cycle was stopped (Fig. 2a and b). The magnitude of the memory effect was defined as the difference (in mV) between the potential of the maximum of the memory effect bump and the potential at that SOC during the normal cycle (Fig. 2b).

The magnitude of the memory effect (MME) is known to increase with decreased specific surface area.<sup>6</sup> Due to the changes in specific surface area (300, 220 and 210 m<sup>2</sup> g<sup>-1</sup> for TiO<sub>2</sub>\_pristine to TiO<sub>2</sub>\_4 h and TiO<sub>2</sub>\_24 h, respectively), a slight increase in MME was expected from TiO<sub>2</sub>\_pristine to TiO<sub>2</sub>\_4 h, while remaining almost constant between TiO<sub>2</sub>\_4 h and TiO<sub>2</sub>\_24 h. However, the MME showed only a small decrease between TiO<sub>2</sub>\_pristine and TiO<sub>2</sub>\_4 h, but it drastically increased for TiO<sub>2</sub>\_24 h (Fig. 3). This trend in the MME completely matched that of the specific charge (Fig. 2) indicating that the MME is strongly correlated with the kinetics of (de-)intercalation process: the faster the kinetics the smaller the memory effect. In this particular case, the sluggish Li-ion mobility in TiO<sub>2</sub> after H<sub>2</sub> annealing for 24 h was responsible for the significant increase in the MME since the electron conductivity continuously increases upon H<sub>2</sub> annealing.<sup>10</sup> Another commercial anatase TiO<sub>2</sub> with lower specific surface area (95 m<sup>2</sup> g<sup>-1</sup>) was also evaluated. In this case, the influence of the specific

surface area was completely ruled out since it did not change upon annealing. The exact same trend in the MME was observed for TiO<sub>2</sub> with 95 m<sup>2</sup> g<sup>-1</sup> confirming the influence of oxygen vacancies on MME. In addition, for the same annealing time, the MME for smaller surface area TiO<sub>2</sub> (95 m<sup>2</sup> g<sup>-1</sup>) was always higher than that of its homologous sample of higher surface area (300 m<sup>2</sup> g<sup>-1</sup>) confirming the dependency between specific surface area and memory effect. Since it is known that larger particles lead to slower kinetics,<sup>8,9,14,15</sup> the higher memory effect for larger particles can be explained on the basis of their slower kinetics. Also the appearance of the memory effect on Al-doped Li<sub>4</sub>Ti<sub>5</sub>O<sub>12</sub> (pristine Li<sub>4</sub>Ti<sub>5</sub>O<sub>12</sub> does not suffer from any memory effect) can be attributed to the slower Li-ion mobility upon doping.

Regarding the overshoot (small peak in the anodic galvanostatic curves before the plateau, Fig. 2b), the relationship between Li-ion mobility, overshoot and memory effect was found to be highly non-linear and saturate as discussed in ESI† (Fig. S3).

In conclusion, while thermodynamics of materials define whether a Li-ion battery material could suffer from memory effect, kinetic aspects have a great influence on whether the phenomenon is observed or not. In the studied case, the slower kinetics related to hindered Li-ion mobility in TiO<sub>2</sub> is causing an increase of the MME. Other reported observations can now be explained on the basis of the kinetics of (de-)intercalation, such as the dependency between particle size and memory effect or the appearance of memory effect upon doping for pristine Li<sub>4</sub>Ti<sub>5</sub>O<sub>12</sub> and Al-doped Li<sub>4</sub>Ti<sub>5</sub>O<sub>12</sub>.

## References

- 1 D. Linden, T. B. Reddy, *Handbook of Batteries*, McGraw-Hill, New York, 2002, pp. 28–18, ISBN 0-07-135978-8.
- 2 R. A. Huggins, *Solid State Ionics*, 2006, **177**, 2643.
- 3 Y. Sato, S. Takeuchi and K. Kobayakawa, *J. Power Sources*, 2001, **93**, 20.
- 4 Y. Nishi, *J. Power Sources*, 2001, **100**, 101.
- 5 T. Sasaki, Y. Ukyo and P. Novak, *Nat. Mater.*, 2013, **12**, 569.
- 6 E. Madej, F. La Mantia, W. Schuhmann and E. Ventosa, *Adv. Energy Mater.*, 2014, **4**, 1400829.
- 7 D. Li, Y. Sun, X. Liu, R. Peng and H. Zhou, *Chem. Sci.*, 2015, **6**, 4066.
- 8 Z. Chen, I. Belharouak, Y.-K. Sun and K. Amine, *Adv. Funct. Mater.*, 2013, **23**, 959.
- 9 M. Fehse and E. Ventosa, *ChemPlusChem*, 2015, **80**, 785.
- 10 J.-Y. Shin, J. H. Joo, D. Samuelis and J. Maier, *Chem. Mater.*, 2012, **24**, 543.
- 11 E. Ventosa, W. Xia, S. Klink, F. La Mantia, B. Mei, M. Muhler and W. Schuhmann, *Chem. – Eur. J.*, 2013, **19**, 14194.
- 12 T. Xia, W. Zhang, J. B. Murowchick, G. Liu and X. Chen, *Adv. Energy Mater.*, 2013, **3**, 1516.
- 13 E. Ventosa, A. Tymoczko, K. Xie, W. Xia, M. Muhler and W. Schuhmann, *ChemSusChem*, 2014, **7**, 2584.
- 14 M. Wagemaker, W. J. H. Borghols and F. M. Mulder, *J. Am. Chem. Soc.*, 2007, **129**, 4323.
- 15 C. Jiang, M. Wei, Z. Qi, T. Kudo, I. Honma and H. Zhou, *J. Power Sources*, 2007, **166**, 239.

